

# Performance evaluation of a shock wave-based method for supersonic bullet trajectory estimation

Kam W. Lo

Maritime Division, Defence Science & Technology Group, 13 Garden Street, Eveleigh, NSW 2015, Australia

## ABSTRACT

The supersonic flight of a bullet generates a ballistic shock wave (SW). As the bullet is subjected to both drag and gravity, its speed decreases with the distance travelled and its trajectory is more or less curvilinear. Given the drag coefficient exponent and the ballistic constant of the bullet, its curvilinear trajectory is specified by five parameters. In this paper, these five parameters are estimated using a SW-based method, which utilizes differential time of arrival (DTOA) of SW measurements from an acoustic sensor array and assumes a linear trajectory, a drag coefficient exponent of 0.5, and a known ballistic constant for the bullet. The point of fire is then located by tracing the estimated curvilinear trajectory of the bullet backwards until it intercepts some obstruction on a digital map. The performance of the SW-based method is evaluated using simulated DTOA data for 36 different types of real bullets, which are generated using Doppler radar measured speeds of the bullets with the gravity taken into account. The standard deviation in the estimates of each parameter is compared with the Cramer-Rao lower bound. The effect of using an erroneous ballistic constant on the performance of the SW-based method is studied.

## 1 INTRODUCTION

When a bullet is fired at supersonic speed, a ballistic shock wave (SW) is generated by the supersonic flight of the bullet (Lo and Ferguson 2012, Maher 2007). The trajectory of the supersonic bullet can be estimated using SW arrivals at an array of acoustic sensors or a network of sensor nodes (each consisting of a small acoustic sensor array). Typical applications of supersonic bullet trajectory estimation include acoustic hit indicators (or target scoring systems) (Cannella, Cappa, and Sciuto 2003, Levanon 2001) and counter-sniper systems (Duckworth, Gilbert, and Barger 1997, Lo 2016). Most of the existing methods for supersonic bullet trajectory estimation simply assume that the speed of the bullet is constant (Cannella, Cappa, and Sciuto 2003, Levanon 2001). A few (more advanced) methods use an exterior ballistic model to account for the deceleration of the bullet due to drag force as it travels along its trajectory (Duckworth, Gilbert, and Barger 1997, Lo 2016). All these methods were formulated with the assumption of a linear bullet trajectory. However, in practice, the bullet trajectory is more or less curvilinear due to gravity. The curvilinear trajectory of a supersonic bullet in the three-dimensional space can be specified by seven parameters: the two coordinates of a reference point on the trajectory, the elevation and azimuth angles of the reversed velocity vector of the bullet and its speed at the reference point, the drag coefficient exponent and the ballistic constant of the bullet (Lo 2017). A model for the differential time of arrival (DTOA) of the SW at a pair of acoustic sensors was derived for a given bullet trajectory (Lo 2017). Assuming a drag coefficient exponent of 0.5, the DTOA model was used to develop a nonlinear least-squares (NLS) method to estimate the other six trajectory parameters using DTOA of SW measurements from each node of an asynchronous sensor network (Lo 2017). This method requires the sensor nodes to be distributed along (and on both sides of) the bullet trajectory and is suitable for ground-based counter-sniper systems for area protection. The method is not applicable to target scoring systems and platform-based counter-sniper systems that use an acoustic sensor array located on the target or platform for bullet trajectory estimation. However, if the ballistic constant of the bullet is also known, then it is possible to estimate the remaining five trajectory parameters using an acoustic sensor array. Moreover, if all the sensors of the array are located not too far away from the reference point, it can be shown using the DTOA model (Lo 2017) that the DTOA of the SW at each sensor pair of the array can be predicted accurately with the assumption of a linear bullet trajectory (which is tangential to the actual curvilinear trajectory at the reference point), and so the gravity can be ignored in the trajectory parameter estimation. In this paper, a SW-based method (Lo 2016), which utilizes DTOA of SW measurements from an acoustic sensor array and assumes a *linear* bullet trajectory, a drag coefficient exponent of 0.5, and a known ballistic constant for the bullet, is used to estimate the remaining five trajectory parameters. The point of fire is then located by tracing the estimated *curvilinear* trajectory of the bullet backwards (taking into account the gravity) until it intercepts some topographic or man-made obstruction on a digital map. The performance of this SW-based method was evaluated previously for the two dimensional case using simulated DTOA data that were generated without taking the gravity into account (Lo 2016). In this paper, its performance is evaluated for the three dimensional case using simulated

DTOA data for 36 different types of real bullets (which are manufactured for a variety of activities including sports shooting, hunting, national defence, and law enforcement), and the DTOA data are generated using Doppler radar measured speeds of the bullets with the gravity taken into account. The standard deviation in the estimates of each parameter is compared with the Cramer-Rao lower bound, and the effect of using an erroneous ballistic constant on the performance of the SW-based method is studied.

## 2 CURVILINEAR TRAJECTORY MODEL FOR A SUPERSONIC BULLET

Figure 1 shows a schematic diagram for the curvilinear trajectory of a supersonic bullet and an acoustic sensor  $S_n$ . The bullet is subjected to drag and gravity as it travels along the trajectory; transverse aerodynamic forces and crosswind drift are ignored. The trajectory lies on the  $xz$ -plane, where  $x$  and  $z$  denote the horizontal and vertical displacements of the bullet, respectively. The point of fire (denoted by  $G$ ) is located at  $x=0$  and  $z=0$ . The bullet is fired at time  $t=0$  with a muzzle speed  $V_0$  at an elevation (or depression) angle  $\theta_0$  (measured relative to  $x$ -axis). At time  $t=t_r$ , the trajectory passes through a reference point  $Q$  at  $x=r$  and  $z=z_r$ , where the speed of the bullet is  $V_r$  and the elevation (or depression) angle of the bullet velocity vector is  $\theta_r$  (measured relative to  $x$ -axis). A curvilinear trajectory model for the supersonic bullet in  $(X, Y, Z)$  coordinates has been derived (Lo 2017). In Fig. 1, the vertical  $xz$ -plane that contains the bullet trajectory is perpendicular to the  $XY$ -plane, with the  $z$ -axis parallel to the  $Z$ -axis. The position vectors of the two points  $G$  and  $Q$  in  $(X, Y, Z)$  coordinates are given by  $\mathbf{R}_G = [X_G, Y_G, Z_G]^T$  and  $\mathbf{R}_Q = [0, Y_Q, Z_Q]^T$ , respectively, where the superscript  $T$  denotes vector transpose. Let  $x'$  denote the horizontal displacement of the bullet from point  $Q$ , and  $z'(x')$  denote the corresponding vertical displacement of the bullet from point  $Q$ . Let  $\phi'_r$  (measured relative to  $X$ -axis) and  $\theta'_r$  (measured relative to  $x'$ -axis) denote the azimuth angle and the elevation (or depression) angle of the *reversed* velocity vector of the bullet at point  $Q$ , respectively. Note that  $\theta'_r = -\theta_r$  and  $\phi'_r$  is the same as the azimuth angle of the relative position vector  $\mathbf{R}_G - \mathbf{R}_Q$ . The bullet's position vector at  $x'$  is given by (Lo 2017)

$$\mathbf{S}'(x') = \mathbf{R}_Q + [x' \cos \phi'_r, x' \sin \phi'_r, z'(x')]^T, \quad (1)$$

where

$$z'(x') = x' \tan \theta'_r + z'_g(x'), \quad (2)$$

$$z'_g(x') = \frac{-g}{2(\eta-1)(\eta-2)} \left( \frac{dV}{ds} \right)_r^{-2} \left( \left[ \frac{\tilde{V}'(x')}{V_r} \right]^{2(\eta-1)} - \frac{2(\eta-1)}{\eta} \left[ \frac{\tilde{V}'(x')}{V_r} \right]^\eta + \frac{\eta-2}{\eta} \right), \quad \eta \neq 0, 1, 2, \quad (3)$$

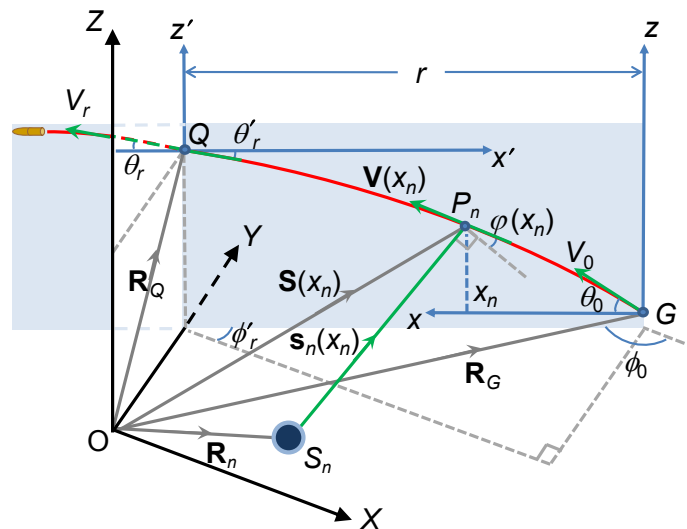


Figure 1: Schematic diagram for the curvilinear trajectory of a supersonic bullet and an acoustic sensor  $S_n$ .

$$\frac{\tilde{V}'(x')}{V_r} = \left[ 1 - \eta \left( \frac{dV}{ds} \right)_r \frac{x'}{V_r \cos \theta'_r} \right]^{\frac{1}{\eta}}, \quad \eta \neq 0, \quad (4)$$

$$\left( \frac{dV}{ds} \right)_r = -\frac{2V_r^{1-\eta}}{C_b}. \quad (5)$$

In (3)–(5),  $g$  is the gravitational acceleration ( $\sim 9.8 \text{ m/s}^2$  at sea level),  $\eta$  and  $C_b$  are the drag coefficient exponent and the ballistic constant of the bullet, respectively, and  $(dV/ds)_r$  is the retardation of the bullet (defined as the derivative of the speed  $V$  of the bullet with respect to the arc length  $s$  along its trajectory) at point  $Q$  (Lo 2017). Equations (1)–(5) constitute a curvilinear trajectory model in  $(X, Y, Z)$  coordinates for a flat-fire, high-velocity supersonic bullet ( $\eta \neq 0, 1, 2$ ). With this model, the bullet trajectory in the three-dimensional space is specified by seven parameters:  $\theta'_r$ ,  $\phi'_r$ ,  $Y_Q$ ,  $Z_Q$ ,  $V_r$ ,  $C_b$ , and  $\eta$ .

### 3 SW-BASED BULLET TRAJECTORY ESTIMATION METHOD

In this paper any quantity with a caret  $\hat{\cdot}$  overhead represents an estimate of that quantity. Consider an array of  $N$  acoustic sensors  $S_1$  to  $S_N$  located around point  $Q$ , and define the parameter vector  $\boldsymbol{\lambda} = [\theta'_r, \phi'_r, Y_Q, Z_Q, V_r]^T$ . Let  $\tau_{k1}$  denote the DTOA of the SW at  $S_k$  and  $S_1$ , which is equal to the SW arrival time at  $S_k$  minus that at  $S_1$ , and  $\tau_{k1}$  is a function of  $\{\boldsymbol{\lambda}, C_b, \eta\}$ , for  $2 \leq k \leq N$ . In the presence of additive measurement errors, the DTOA estimates for the  $(N-1)$  pairs of sensors can be written in vector form as

$$\hat{\mathbf{b}} = \mathbf{b}(\boldsymbol{\lambda}, C_b, \eta) + \mathbf{n}, \quad (6)$$

where  $\hat{\mathbf{b}} = [\hat{\tau}_{21}, \hat{\tau}_{31}, \dots, \hat{\tau}_{N1}]^T$ ,  $\mathbf{b} = [\tau_{21}, \tau_{31}, \dots, \tau_{N1}]^T$ , and  $\mathbf{n} = [n_1, n_2, \dots, n_{N-1}]^T$  are the DTOA observation vector, DTOA model vector, and DTOA observation error vector, respectively. The objective is to estimate  $\boldsymbol{\lambda}$ , given the time delay observation vector  $\hat{\mathbf{b}}$  together with the drag coefficient exponent  $\eta$  and the ballistic constant  $C_b$  of the bullet. A SW-based method (Lo 2016), which was formulated with the assumption of a linear bullet trajectory (by ignoring the gravity), a drag coefficient exponent  $\bar{\eta} = 0.5$ , and an estimated (or presumed) ballistic constant  $\hat{C}_b$  for the bullet, is used to estimate  $\boldsymbol{\lambda}$ . The method adopts a (weighted) NLS approach with the simplifying assumption that the measurement error for the SW arrival time at each sensor is independent, zero-mean, Gaussian distributed with a standard deviation (SD)  $\sigma$ . The NLS estimate of  $\boldsymbol{\lambda}$  is given by (Lo 2016)

$$\hat{\boldsymbol{\lambda}} = \arg \min_{\boldsymbol{\lambda}} [\hat{\mathbf{b}} - \mathbf{b}(\boldsymbol{\lambda}', \hat{C}_b, \bar{\eta})]^T \bar{\mathbf{N}}^{-1} [\hat{\mathbf{b}} - \mathbf{b}(\boldsymbol{\lambda}', \hat{C}_b, \bar{\eta})], \quad (7)$$

where  $\bar{\mathbf{N}} = \sigma^2(\mathbf{I} + \mathbf{E})$  is the covariance matrix of  $\mathbf{n}$  under the simplifying assumption, in which  $\mathbf{I}$  is the  $(N-1) \times (N-1)$  identity matrix and  $\mathbf{E}$  is the  $(N-1) \times (N-1)$  unit matrix consisting of ones. (The constant  $\sigma^2$  in the assumed error covariance matrix  $\bar{\mathbf{N}}$  can be omitted when  $\bar{\mathbf{N}}$  is used in (7) to compute  $\hat{\boldsymbol{\lambda}}$ .) The DTOA model vector  $\mathbf{b}$  in (7) is computed by ignoring the gravity (assuming a linear bullet trajectory). An efficient computation method for  $\mathbf{b}$  can be found in a previous paper (Lo 2016).

Once  $\hat{\boldsymbol{\lambda}} = [\hat{\theta}'_r, \hat{\phi}'_r, \hat{Y}_Q, \hat{Z}_Q, \hat{V}_r]^T$  are obtained using (7), the curvilinear trajectory of the bullet can be estimated using (1)–(5). The position of the shooter can be determined by tracing the estimated curvilinear trajectory of the bullet backwards until it intercepts some obstruction. This paper simply assumes that the  $Z$ -coordinate  $Z_G$  of the shooter is known. In this case, the  $X$ - and  $Y$ -coordinates  $(X_G, Y_G)$  of the shooter can be estimated as follows. Since  $\mathbf{S}'(x') = \mathbf{R}_G$  at  $x' = r$ , it follows from (1) and (2) that

$$X_G = r \cos \phi'_r, \quad Y_G = Y_Q + r \sin \phi'_r, \quad (8)$$

$$Z_G = Z_Q + r \tan \theta'_r + z'_g(r). \quad (9)$$

Substituting  $\{\hat{\theta}_r', \hat{Z}_Q, \hat{V}_r, \hat{C}_b, \hat{\eta}\}$  for  $\{\theta_r', Z_Q, V_r, C_b, \eta\}$  in (9) and solving the resulting nonlinear equation of  $r$  gives  $\hat{r}$ . Substituting  $\{\hat{r}, \hat{Y}_Q, \hat{\phi}_r'\}$  for  $\{r, Y_Q, \phi_r'\}$  in (8) then gives  $\{\hat{X}_G, \hat{Y}_G\}$ .

#### 4 GENERATION OF SIMULATED DTOA MEASUREMENT VECTOR

Refer to Fig. 1. Let  $v_x$  and  $v_z$  denote the  $x$ - and  $z$ -components of the bullet velocity, respectively, and  $\phi_0$  denote the azimuth angle (measured relative to  $X$ -axis) of the velocity vector of the bullet at point  $G$  (which is the same as the azimuth angle of the relative position vector  $\mathbf{R}_Q - \mathbf{R}_G$ ). The bullet's velocity and position vectors at  $x$  are given, respectively, by (Lo 2017)

$$\mathbf{V}(x) = [v_x(x) \cos \phi_0, v_x(x) \sin \phi_0, v_z(x)]^T, \quad (10)$$

$$\mathbf{S}(x) = \mathbf{R}_G + [x \cos \phi_0, x \sin \phi_0, z(x)]^T, \quad (11)$$

where

$$v_x(x) = \bar{V}(x) \cos \theta_0, \quad v_z(x) = \bar{V}(x) \sin \theta_0 + v_z^P(x), \quad z(x) = x \tan \theta_0 + z^P(x), \quad (12)$$

$$v_z^P(x) = \frac{-g}{(\eta-2)} \left( \frac{dV}{ds} \right)_0^{-1} \left( \left[ \frac{\bar{V}(x)}{V_0} \right]^{\eta-1} - \left[ \frac{\bar{V}(x)}{V_0} \right] \right), \quad \eta \neq 0, 1, 2, \quad (13)$$

$$z^P(x) = \frac{-g}{2(\eta-1)(\eta-2)} \left( \frac{dV}{ds} \right)_0^{-2} \left( \left[ \frac{\bar{V}(x)}{V_0} \right]^{2(\eta-1)} - \frac{2(\eta-1)}{\eta} \left[ \frac{\bar{V}(x)}{V_0} \right]^{\eta} + \frac{\eta-2}{\eta} \right), \quad \eta \neq 0, 1, 2, \quad (14)$$

$$\frac{\bar{V}(x)}{V_0} = \left[ 1 + \eta \left( \frac{dV}{ds} \right)_0 \frac{x}{V_0 \cos \theta_0} \right]^{\frac{1}{\eta}}, \quad \eta \neq 0, \quad (15)$$

$$\left( \frac{dV}{ds} \right)_0 = -\frac{2V_0^{1-\eta}}{C_b}. \quad (16)$$

The time required for the bullet to travel to a horizontal range  $x$  from the point of fire  $G$  is given by (Lo 2017)

$$t(x) = \frac{1}{(\eta-1)} \left( \frac{dV}{ds} \right)_0^{-1} \left( \left[ \frac{\bar{V}(x)}{V_0} \right]^{\eta-1} - 1 \right), \quad \eta \neq 0, 1. \quad (17)$$

In (13)–(16),  $(dV/ds)_0$  is the retardation of the bullet at the muzzle (or point of fire  $G$ ). Let  $P_n$  denote the detach point of SW for sensor  $S_n$ , for  $1 \leq n \leq N$ . Since the Mach cone angle  $\varphi(x)$  is related to the speed  $V(x)$  of the bullet by  $\sin \varphi(x) = c/V(x)$ , the horizontal range  $x_n$  (from point  $G$ ) of  $P_n$  can be obtained by finding the solution to the following nonlinear equation of  $x$  (Lo 2017):

$$\mathbf{s}_n(x)^T \mathbf{V}(x) = -c s_n(x) \quad \text{at } x = x_n, \quad (18)$$

where  $\mathbf{s}_n(x) = \mathbf{S}(x) - \mathbf{R}_n$  and  $s_n(x) = \|\mathbf{s}_n(x)\|$  ( $\|\cdot\|$  denotes  $L_2$  norm of a vector). The arrival time  $\tau_n$  of the SW at  $S_n$  is given by

$$\tau_n = t(x_n) + s_n(x_n)/c, \quad 1 \leq n \leq N. \quad (19)$$

The DTOA of the SW at  $S_k$  and  $S_1$  is given by  $\tau_{k1} = \tau_k - \tau_1$ , for  $2 \leq k \leq N$ . Given the coordinates of the point of fire  $G (X_G, Y_G, Z_G)$  and the reference point  $Q (0, Y_Q, Z_Q)$ , and the drag coefficient exponent  $\eta$ , the muzzle speed  $V_0$ , and the ballistic constant  $C_b$  of the bullet, then the azimuth angle  $\phi_0$  and the elevation (or depression) angle  $\theta_0$  of the velocity vector of the bullet at point  $G$ , the azimuth angle  $\phi'_r$  and the elevation (or depression) angle  $\theta'_r$  of the reversed velocity vector of the bullet at point  $Q$ , and the speed  $V_r$  of the bullet at point  $Q$  can be obtained using (12)–(16). The arrival time of the SW at each sensor is computed using (19) with the aid of (10)–(18). Independent, zero-mean, Gaussian random numbers (white Gaussian noise) with a standard deviation of  $\sigma$  are then added to the computed SW arrival times. (In practice, the SW arrival time at each sensor is estimated by applying an edge detector (Sadler, Pham, and Sadler 1998) to the sensor output signal.) The simulated DTOA measurement vector is generated by subtracting the noisy SW arrival time at sensor 1 from the noisy SW arrival times at the other sensors of the array.

## 5 SIMULATIONS

Thirty six different types of real bullets (Lo and Ferguson 2016), with calibers ranging from 5.56 mm to 12.95 mm, were used in the simulations. Doppler radar measured speed data are available for each of these bullet types. For flat fire, the speed profile (the variation with distance  $x$  of the speed) of a supersonic bullet is described accurately by (Lo and Ferguson 2016)

$$V(x) = (V_0^\eta - 2\eta C_b^{-1}x)^{1/\eta}. \quad (20)$$

For a given bullet type, Eq. (20) (referred to as the general speed model) was fitted to the corresponding radar measured speed data in a least-squares (LS) sense by adjusting the values of  $\{V_0, C_b, \eta\}$ , and the set of parameters values that provides the LS fit is denoted as  $\{V_0^*, C_b^*, \eta^*\}$ . The range of  $\eta^*$  is about 0.2–0.73 over all 36 bullet types. Similarly, the set of values of  $\{V_0, C_b\}$  that provides a LS fit of Eq. (20) with  $\eta$  fixed at  $\bar{\eta} = 0.5$  (referred to as the quadratic speed model) to the radar measured speed data is denoted as  $\{\bar{V}_0, \bar{C}_b\}$ . Figure 2 shows the quadratic speed model parameters  $\{\bar{V}_0, \bar{C}_b\}$  for each bullet type. Note that the 36 bullet types have been arranged in ascending order of  $\bar{C}_b$ . The root-mean-square (RMS) deviation of the LS fit of each speed model from the radar measured speed data for each bullet type was published in a previous paper (Lo 2017) where the 36 bullet types were arranged in ascending order of  $\eta^*$ . The RMS deviations (or errors) range from about 0.1 to 4 m/s for the general speed model and 0.3 to 9.1 m/s for the quadratic speed model over all 36 bullet types. Comparing the two models, the general speed model predicts more accurately the speed profile for each bullet type, especially when  $\eta^*$  deviates further from 0.5. Here, the parameter values  $\{V_0^*, C_b^*, \eta^*\}$  for the general speed model were treated as the ‘actual values’ of  $\{V_0, C_b, \eta\}$  and used to generate the simulated DTOA measurement vector (using the method described in Section 4), which was then processed using the SW-based method (7).

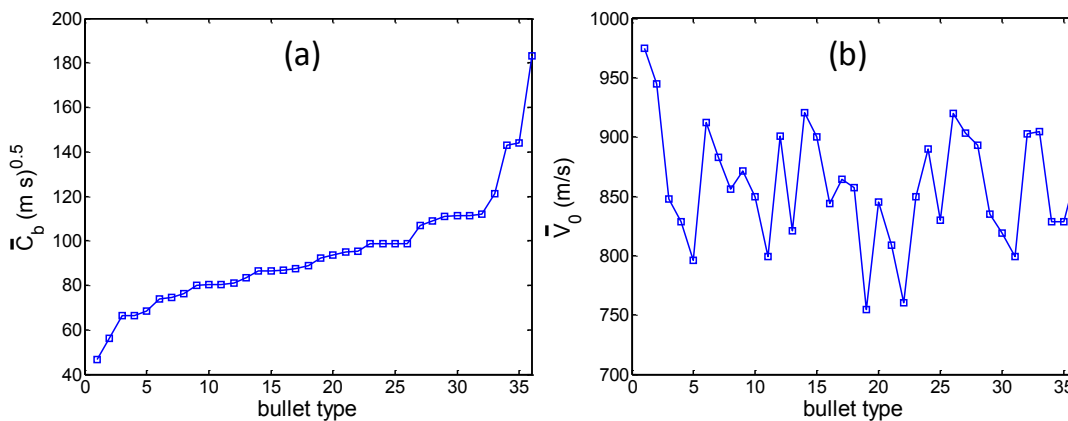


Figure 2: Quadratic speed model parameters  $\{\bar{V}_0, \bar{C}_b\}$  for each bullet type.

Computer simulations were carried out in MATLAB<sup>®</sup>. The acoustic array used in the simulations consisted of 9 sensors whose  $(X, Y, Z)$  coordinates in meters were  $(0, 0, -1.5)$ ,  $(0, -2, -1.5)$ ,  $(0, 2, -1.5)$ ,  $(0, -1, 1.5)$ ,  $(0, 1, 1.5)$ ,  $(0.1, -3, 1.5)$ ,  $(0.1, 3, 1.5)$ ,  $(0.2, -3, -1.5)$ , and  $(0.2, 3, -1.5)$ , respectively – see Fig. 3(a). The point of fire  $G$  was located at  $(600, 0, -50)$  m and point  $Q$  at  $(0, 2, 1)$  m. The measurement error for the SW arrival time at each sensor was independent, zero-mean, Gaussian distributed with a SD  $\sigma$  equal to  $10 \mu\text{s}$  (corresponding to a measurement error SD of  $10\sqrt{2} \mu\text{s}$  for the DTOA of the SW at each sensor pair). The minimization in (7) was performed using the MATLAB optimization function *lsqnonlin*. The initial estimates of  $\{\theta'_r, \phi'_r, Y_Q, Z_Q, V_r\}$  were set equal to  $\{0, 0, 1, 0, 1.5c\}$ . A total of 100 simulations were performed for each bullet type. Figures 3(b)–(d) show, respectively, the estimates of  $\{\phi'_r, \theta'_r\}$ ,  $\{Y_Q, Z_Q\}$ , and  $\{X_G, Y_G\}$  obtained using the SW-based method with  $\hat{C}_b = \bar{C}_b$  for all 100 simulations and the corresponding Cramer-Rao lower bounds (CRLBs) for bullet type 22. The CRLBs on the covariance matrices for  $\hat{\lambda}$  and  $\{\hat{X}_G, \hat{Y}_G\}$  were computed, respectively, as (Lo 2017)

$$\mathbf{Q} = [\nabla \mathbf{b}^T \bar{\mathbf{N}}^{-1} (\nabla \mathbf{b}^T)^T]^{-1}, \quad \mathbf{C} = \mathbf{H} \mathbf{Q} \mathbf{H}^T, \quad (21)$$

where  $\nabla = [\partial/\partial\theta'_r, \partial/\partial\phi'_r, \partial/\partial Y_Q, \partial/\partial Z_Q, \partial/\partial V_r]^T$  is the gradient operator,  $\mathbf{H}^T = \nabla[X_G, Y_G]$ , and both  $\mathbf{H}^T$  and  $\nabla \mathbf{b}^T$  were evaluated at  $\{\hat{\lambda}, \bar{C}_b, \bar{\eta}\}$ . It can be seen from Figs. 3(b)–(d) that with the SW-based method, the bias errors are small and the one-SD ellipses closely match the corresponding CRLB ellipses (which is expected as the NLS estimates are the maximum likelihood estimates under the white Gaussian noise assumption). Also shown in Fig. 3(d) for comparison purposes are the estimates of the point of fire position obtained using (8) and (9) with the gravity or the last term  $z'_g(r)$  in (9) ignored (equivalent to tracing an estimated *linear* bullet trajectory backwards), which results in large bias errors.

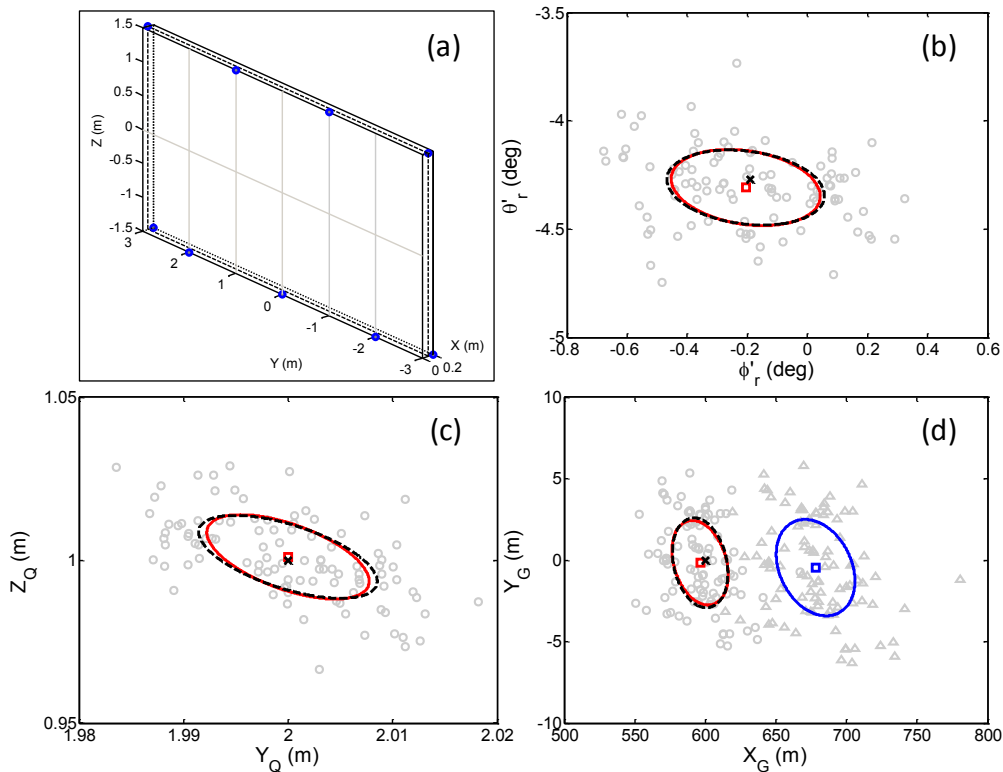


Figure 3: (a) Sensor configuration (circles denote sensor positions). (b)–(d) Simulation results obtained using the SW-based method with  $\hat{C}_b = \bar{C}_b$  for bullet type 22 when  $\mathbf{R}_G = [600, 0, -50]^T$  m and  $\mathbf{R}_Q = [0, 2, 1]^T$  m (circles denote estimates from the SW-based method, triangles in (d) denote estimates of the point of fire position obtained by tracing an estimated linear bullet trajectory backwards, squares denote mean values of estimates, cross denote actual values, solid lines denote one-SD ellipses, and dashed lines denote CRLB ellipses).

Figure 4 shows the bias errors (denoted by diamonds) and SDs (denoted by squares) in the estimates of  $\{\theta'_r, \phi'_r, Y_Q, Z_Q, X_G, Y_G\}$  obtained using the SW-based method with  $\hat{C}_b = \bar{C}_b$  and the corresponding CRLBs (denoted by circles) for all 36 bullet types. It can be observed from Fig. 4 that the SDs match quite well the CRLBs and the bias errors are small for all 36 bullet types. To study the effect of using an erroneous ballistic constant ( $\hat{C}_b \neq \bar{C}_b$ ) on the performance of the SW-based method, simulations were performed in turn with  $\hat{C}_b = 60, 90, 120,$  and  $10^4$   $(\text{m s})^{0.5}$  (in the last case the speed of the bullet is approximately constant over its flight path to point Q). Figures 5 and 6 show the bias errors and SDs in the estimates of  $\{\theta'_r, \phi'_r, Y_Q, Z_Q, X_G, Y_G\}$  obtained using the SW-based method with  $\hat{C}_b = 120(\text{m s})^{0.5}$  and  $\hat{C}_b = 10^4$   $(\text{m s})^{0.5}$ , respectively, and the corresponding CRLBs for all 36 bullet types. It is expected that the bias error of a parameter estimate increases as  $\hat{C}_b$  deviates further from  $\bar{C}_b$ , and this trend is clearly observed for  $\{\hat{\theta}'_r, \hat{Z}_Q, \hat{X}_G\}$  in Fig. 6, where  $\hat{C}_b = 10^4$   $(\text{m s})^{0.5}$  and  $\bar{C}_b$  increases with bullet type from approximately 46 to 183  $(\text{m s})^{0.5}$ . The results for bullet type 1 are not as good as those for the other bullet types as can be seen from Figs. 4–6. This is because the ballistic constant  $\bar{C}_b$  for bullet type 1 is too small so that after travelling a long distance ( $\sim 600$  m), the speed  $V_r$  of the bullet at point Q is close to subsonic.

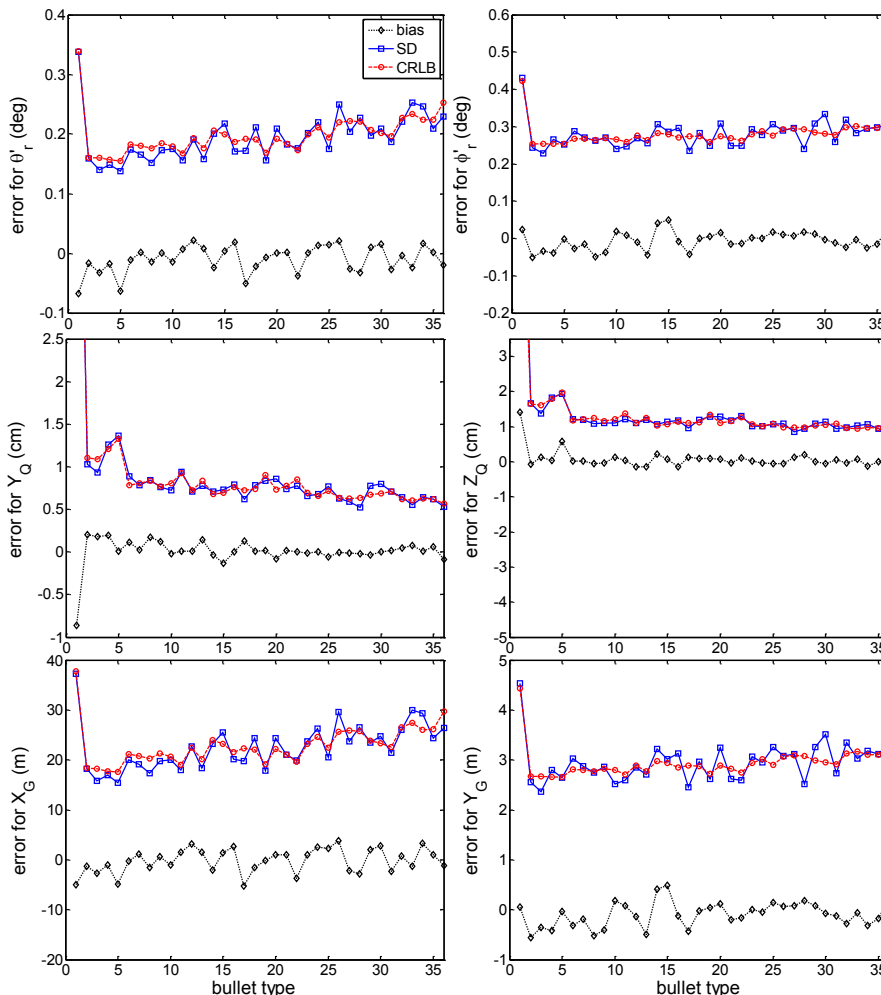


Figure 4: Bias errors (diamonds) and SDs (squares) in the estimates of  $\{\theta'_r, \phi'_r, Y_Q, Z_Q, X_G, Y_G\}$  obtained using the SW-based method with  $\hat{C}_b = \bar{C}_b$   $(\text{m s})^{0.5}$ , and the corresponding CRLBs (circles) for all 36 bullet types, when  $\mathbf{R}_G = [600, 0, -50]^T \text{m}$  and  $\mathbf{R}_Q = [0, 2, 1]^T \text{m}$ .

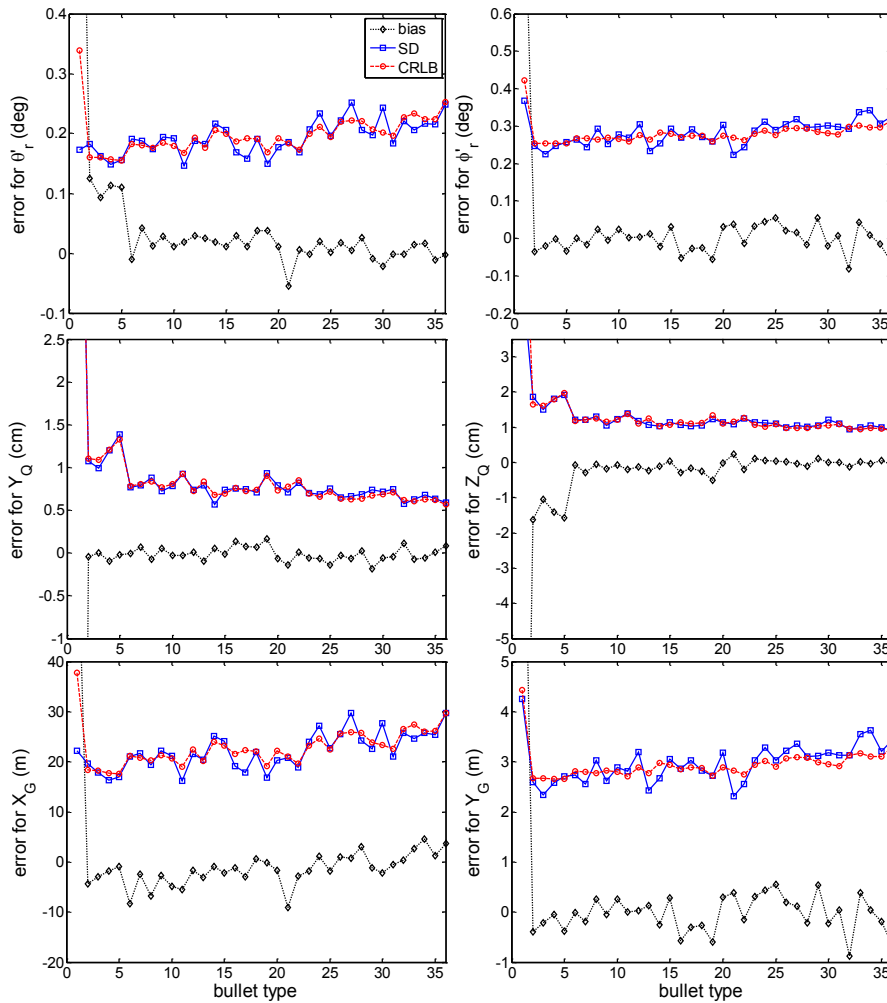


Figure 5: Similar to Fig. 4 but for  $\hat{C}_b = 120 \text{ (m s)}^{0.5}$ .

Bullet type 1 is excluded in the comparison of the results for the five different values of  $\hat{C}_b$ :  $\bar{C}_b$ , 60, 90, 120, and  $10^4 \text{ (m s)}^{0.5}$ . Here, the root mean squared (RMS) bias error for a parameter estimate is defined as the RMS value of the bias errors for that parameter estimate over 35 bullet types 2–36. The RMS SD and RMS CRLB for a parameter estimate are defined in a similar way. Table 1 shows the RMS bias errors, the RMS SDs, and the RMS CRLBs for  $\{\hat{\theta}'_r, \hat{\phi}'_r, \hat{Y}_Q, \hat{Z}_Q, \hat{X}_G, \hat{Y}_G, \hat{V}_r\}$  for the five different values of  $\hat{C}_b$ . It can be observed from Table 1 that the accuracy of  $\{\hat{\theta}'_r, \hat{\phi}'_r, \hat{Y}_Q, \hat{Z}_Q, \hat{X}_G, \hat{Y}_G, \hat{V}_r\}$  is not significantly degraded (in a RMS sense over 35 bullet types) when  $\hat{C}_b$  assumes typical values: 60, 90, and  $120 \text{ (m s)}^{0.5}$  (instead of the correct value  $\bar{C}_b$ ) in the trajectory parameter estimation. Simulations have also been performed for another position of the point of fire: (600, 60, -50) m with point Q staying at (0, 2, 1). In this scenario, the azimuth angle  $\hat{\phi}'_r$  increased to  $5.52^\circ$  (while it was  $-0.19^\circ$  in the previous scenario). Table 2 shows the RMS bias errors, the RMS SDs, and the RMS CRLBs for  $\{\hat{\theta}'_r, \hat{\phi}'_r, \hat{Y}_Q, \hat{Z}_Q, \hat{X}_G, \hat{Y}_G, \hat{V}_r\}$  for the five different values of  $\hat{C}_b$ :  $\bar{C}_b$ , 60, 90, 120, and  $10^4 \text{ (m s)}^{0.5}$ . A similar observation to Table 1 can be made from Table 2.

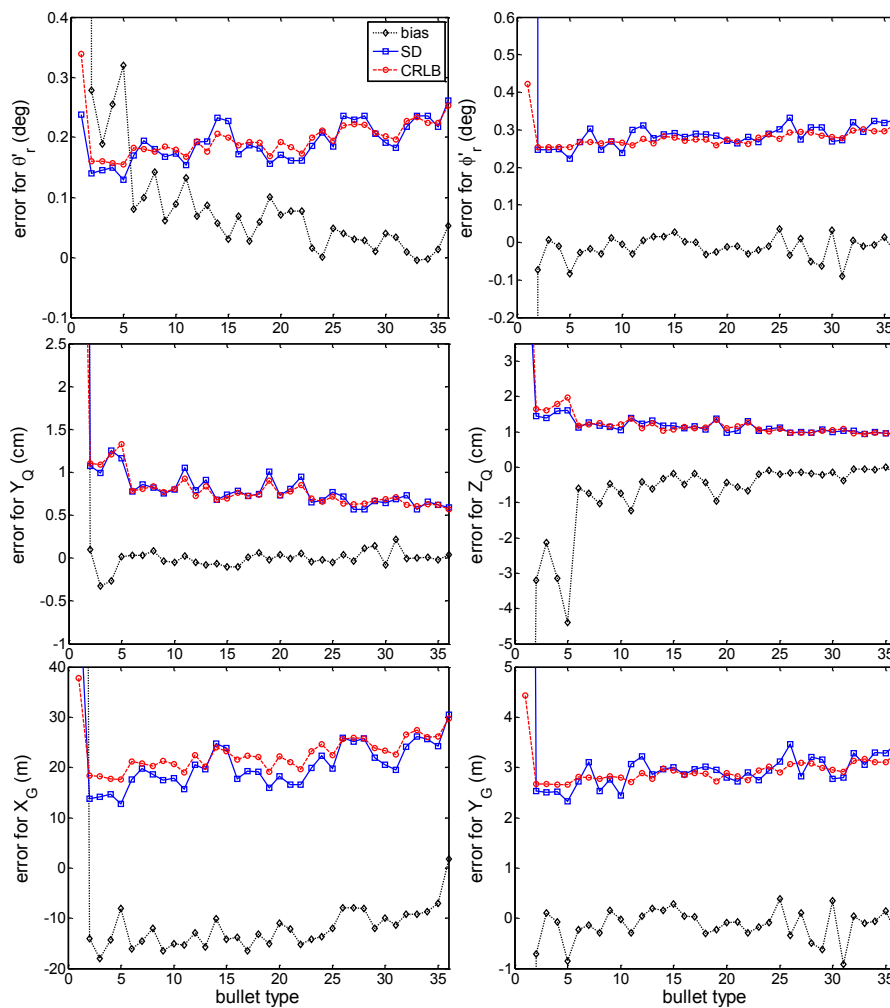


Figure 6: Similar to Fig. 4 but for  $\hat{C}_b = 10^4 \text{ (m s)}^{0.5}$ .

## 6 CONCLUSIONS

A SW-based method for supersonic bullet trajectory estimation has been studied. The method adopts a quadratic speed model for the bullet (corresponding to a drag coefficient exponent  $\bar{\eta}$  of 0.5) and assumes that the ballistic constant  $\bar{C}_b$  of this model is known (or has been correctly estimated) *a priori* and the bullet trajectory is linear (by ignoring the gravity). It uses DTOA of SW measurements from an acoustic sensor array to estimate the five trajectory parameters of the bullet. These estimated parameters are then used to compute the curvilinear trajectory of the bullet (by taking into account the gravity), which is traced backwards to locate the point of fire. The performance of the SW-based method has been evaluated using simulated data for 36 different types of real bullets, and the effect on its performance when the estimated (or presumed) ballistic constant  $\hat{C}_b$  is in error has been studied. Two typical scenarios have been considered for a 9-element 6 m x 3 m x 0.2 m volume sensor array. The point of fire was located at a firing range of 600 m for both scenarios, and the bullet passed through the volume array at the same reference point (0, 2, 1) m at an azimuth angle  $\hat{\phi}_r$  of  $-0.19^\circ$  for the first scenario and  $5.52^\circ$  for the second scenario. The computer simulation results show that when  $\hat{C}_b$  equals the correct value  $\bar{C}_b$ , the bias errors in the parameter estimates (due to the assumption of a linear trajectory and the use of a quadratic speed model) are small and the SDs match quite well the CRLBs. Also, the accuracy of the parameter estimates is not significantly degraded (in a RMS sense over 35 bullet types) when  $\hat{C}_b$  assumes typical values: 60, 90, and 120  $\text{(m s)}^{0.5}$  (instead of the correct value  $\bar{C}_b$ ) in the trajectory parameter estimation.

Table 1: Comparison of results for five different cases:  $\hat{C}_b = \bar{C}_b, 60, 90, 120, \text{ and } 10^4 \text{ (m s)}^{0.5}$ , when  $\mathbf{R}_Q = [0, 2, 1]^T \text{ m}$  and  $\mathbf{R}_G = [600, 0, -50]^T \text{ m}$ . For each of  $\{\hat{\theta}'_r, \hat{\phi}'_r, \hat{Y}_Q, \hat{Z}_Q, \hat{X}_G, \hat{Y}_G, \hat{V}_r\}$ , (1st value, 2nd value) = (RMS bias error, RMS SD).

$\hat{C}_b \text{ (m s)}^{0.5}$	$\hat{\theta}'_r \text{ (}^\circ\text{)}$	$\hat{\phi}'_r \text{ (}^\circ\text{)}$	$\hat{Y}_Q \text{ (cm)}$	$\hat{Z}_Q \text{ (cm)}$	$\hat{X}_G \text{ (m)}$	$\hat{Y}_G \text{ (m)}$	$\hat{V}_r \text{ (m/s)}$
$\bar{C}_b$	(0.02, 0.19)	(0.02, 0.28)	(0.08, 0.79)	(0.14, 1.18)	( 2.30, 22.45)	(0.27, 2.92)	(0.28, 3.54)
60	(0.05, 0.19)	(0.02, 0.28)	(0.09, 0.79)	(0.35, 1.19)	( 4.63, 23.20)	(0.26, 2.95)	(0.87, 3.60)
90	(0.03, 0.19)	(0.03, 0.27)	(0.08, 0.79)	(0.34, 1.19)	( 2.55, 22.85)	(0.31, 2.89)	(0.54, 3.55)
120	(0.04, 0.19)	(0.03, 0.28)	(0.08, 0.80)	(0.51, 1.21)	( 3.40, 22.45)	(0.35, 2.96)	(0.85, 3.70)
$10^4$	(0.11, 0.19)	(0.03, 0.28)	(0.10, 0.80)	(1.22, 1.16)	(12.68, 20.59)	(0.34, 2.93)	(2.07, 3.64)
RMS CRLB	0.19	0.28	0.79	1.20	22.64	2.90	3.53

Table 2: Similar to Table 1 but for  $\mathbf{R}_G = [600, 60, -50]^T \text{ m}$ .

$\hat{C}_b \text{ (m s)}^{0.5}$	$\hat{\theta}'_r \text{ (}^\circ\text{)}$	$\hat{\phi}'_r \text{ (}^\circ\text{)}$	$\hat{Y}_Q \text{ (cm)}$	$\hat{Z}_Q \text{ (cm)}$	$\hat{X}_G \text{ (m)}$	$\hat{Y}_G \text{ (m)}$	$\hat{V}_r \text{ (m/s)}$
$\bar{C}_b$	(0.03, 0.23)	(0.02, 0.26)	(0.09, 0.81)	(0.14, 1.20)	( 2.30, 26.70)	(0.42, 3.57)	(0.24, 3.37)
60	(0.05, 0.23)	(0.02, 0.26)	(0.07, 0.82)	(0.35, 1.25)	( 5.08, 28.00)	(0.57, 3.69)	(0.83, 3.35)
90	(0.04, 0.23)	(0.02, 0.26)	(0.08, 0.83)	(0.31, 1.23)	( 3.73, 27.41)	(0.48, 3.68)	(0.51, 3.39)
120	(0.05, 0.23)	(0.02, 0.26)	(0.08, 0.82)	(0.49, 1.21)	( 3.22, 26.29)	(0.40, 3.58)	(0.71, 3.39)
$10^4$	(0.12, 0.23)	(0.03, 0.26)	(0.06, 0.82)	(1.24, 1.18)	(11.55, 24.34)	(1.22, 3.40)	(1.87, 3.34)
RMS CRLB	0.23	0.26	0.81	1.22	26.74	3.61	3.31

## REFERENCES

- Cannella, M., Cappa, P., and Sciuto, S.A. 2003. 'A novel approach for determining the trajectory and speed of a supersonic object'. *Measurement Science and Technology* 14: 654-662.
- Duckworth, G.L., Gilbert, D.C., and Barger, J.E. 1997. 'Acoustic counter-sniper system'. *Proceedings of SPIE* 2938: 262-275.
- Maher, R.C. 2007. 'Acoustical characterization of gunshots'. In *Proceedings of the IEEE Workshop on Signal Processing Applications for Public Security and Forensics (SAFE'07)*, 109-113.
- Levanon, N. 2001. 'Acoustic hit indicators'. *IEEE Transactions on Aerospace and Electronic Systems* 38 (1): 304-309.
- Lo, K.W. 2016. 'Supersonic bullet trajectory estimation using ballistic shock wave arrivals at an acoustic sensor array'. In *Proceedings of Acoustics 2016*. Brisbane, Australia.
- Lo, K.W. 2017. 'Curvilinear trajectory estimation of a supersonic bullet using ballistic shock wave arrivals at asynchronous acoustic sensor nodes'. *Journal of Acoustical Society of America* 141: 4543-4555.
- Lo, K.W. and Ferguson, B.G. 2012. 'Localization of small arms fire using acoustic measurements of muzzle blast and/or ballistic shock wave arrivals'. *Journal of Acoustical Society of America* 132: 2997-3017.
- Lo, K.W. and Ferguson, B.G. 2016. 'Comparison of supersonic bullet ballistic models for accurate localization of small arms fire'. *IET Radar, Sonar and Navigation* 10: 1536-1540.
- Sadler, B.M., Pham, T., and Sadler, L.C. 1998. 'Optimal and wavelet-based shock wave detection and estimation'. *Journal of Acoustical Society of America* 104: 955-963.